Trajectories of charged particles in the static Ernst space-time

1979 J. Phys. A: Math. Gen. 12 215

(http://iopscience.iop.org/0305-4470/12/2/009)

J. Phys. A: Math. Gen., Vol. 12, No. 2, 1979. Printed in Great Britain

Trajectories of charged particles in the static Ernst space–time

N Dadhich†§, C Hoenselaers‡|| and C V Vishveshwara‡

† Raman Research Institute, Bangalore 560 006, India and Centre for Theoretical Studies, Indian Institute of Science, Bangalore 560 012, India
‡ Raman Research Institute, Bangalore 560 006, India

Received 21 June 1978

Abstract. We study the trajectories of charged particles in Ernst's space–time representing a static black hole immersed in a magnetic field. We find bound orbits always exist for realistic magnetic field strengths. A similar investigation is carried out for the case of Melvin's magnetic universe and for a corresponding test field superposed on a flat space–time.

1. Introduction

There has been considerable interest in the study of electromagnetic fields and motion of charged particles in curved space–times. Several authors, too numerous to mention here, have considered this problem. In this paper we shall study the motion of charged particles in Ernst's static space–time (Ernst 1976), which represents a Schwarschild black hole immersed in an axially symmetric magnetic field which becomes uniform asymptotically if $|Bm| \ll 1$.

A situation like this (a black hole embedded in an external magnetic field) may occur in the realm of astrophysics. Our calculations would be of relevance if the magnetic field is sufficiently strong.

In the next section, we given Ernst's metric and work out trajectories of particles using the Hamilton–Jacobi equation (Carter 1968). Melvin's magnetic universe (Melvin 1964) is also studied in a similar fashion. Finally, in § 3, we discuss the energy curves together with lines of constant potential and magnetic field lines for Ernst's space–time. The energy curves for Melvin's universe are compared with those for a corresponding test field superposed on a flat background.

2. Ernst's metric and trajectories

Ernst's metric is given by

$$ds^2 = \lambda^2[(1-2mr^{-1})^{-1}\,dr^2 + r^2\,d\theta^2 - (1-2mr^{-1})\,dt^2] + (r^2\sin^2\theta/\lambda^2)\,d\phi^2 \tag{1}$$

$$\lambda = 1 + B^2r^2\sin^2\theta \tag{2}$$

$$\Phi \equiv A_i\eta^i = Br^2\sin^2\theta/\lambda \tag{3}$$

§ Visiting from the Department of Mathematics, University of Poona, Poona 411 007, India.
|| Present address: Department of Physics, Montana State University, Montana 59715, USA.

0305-4470/79/020215+07$01.00

where Φ is the electric potential with respect to the angular Killing vector η^i $(\partial\phi)$, A_i is the four-potential and B is the constant value of the magnetic field on the axis. As usual we have set $G = c = 1$.

The metric (1) reduces to Schwarzschild's metric for $\lambda = 1$, to Melvin's magnetic universe (Melvin 1964) for $m = 0$ and to the test field superposed on flat space–time for $\lambda = 1$ (only in (1)) and $m = 0$.

It should be kept in mind that the electric and magnetic potentials with respect to a Killing vector ξ are defined by

$$\nabla_i \Phi_E = F_{ij}\xi^j \qquad \nabla_i \Phi_M = {}^*F_{ij}\xi^j \tag{4}$$

respectively. F_{ij} is the electromagnetic field tensor and ${}^*F_{ij}$ is its conjugate. So one finds that the electric potential for the ∂t Killing vector vanishes and the magnetic one is given by

$$\Phi_M = 2B\cos\theta(r - 2m). \tag{5}$$

The magnetic field lines will be orthogonal to the constant lines and hence their equation reads

$$r\sin\theta = \text{constant}. \tag{6}$$

Following Carter (1968), we write the Hamilton–Jacobi equation

$$S_{,\tau} \equiv \frac{\partial S}{\partial \tau} = \tfrac{1}{2} g^{ij}(S_{,i} - eA_i)(S_{,j} - eA_j) \tag{7}$$

for a particle of mass μ and charge e as

$$-\mu^2 = \lambda^{-2}(1 - 2mr^{-1})(S_{,r})^2 + \lambda^{-2} r^{-2}(S_{,\theta})^2 + \lambda^2 r^{-2}\sin^{-2}\theta(S_{,\phi} - e\Phi)^2 - \lambda^{-2}(1 - 2mr^{-1})^{-1}(S_{,t})^2. \tag{8}$$

One can readily write the energy and the axial angular momentum of the particle as

$$-S_{,t} \equiv -p_t \equiv \epsilon = \lambda^2(1 - 2mr^{-1})\dot{t} \tag{9}$$

$$S_{,\phi} \equiv p_\phi + e\Phi \equiv l = r^2\sin^2\theta\dot{\phi} + e\Phi. \tag{10}$$

Here and in what follows an overhead dot denotes differentiation with respect to the proper time τ. The Hamilton–Jacobi equation is unfortunately not separable in this case. However, we can write the Jacobi action in the form

$$S = S(r, \theta) + l\phi - \epsilon t - \tfrac{1}{2}\mu^2\tau. \tag{11}$$

We see from symmetry considerations that motion confined to the equatorial plane exists and so we consider such motion by setting $\theta = \frac{1}{2}\pi$ and $p_\theta = 0$ in (8), which now becomes separable.

Now $S(r, \theta) = S(r)$ and is given by

$$S(r) = \int \frac{(\epsilon^2 - R)^{1/2}}{1 - 2mr^{-1}}\,\mathrm{d}r, \tag{12}$$

which implies

$$\epsilon^2 \geqslant R \equiv \lambda^2(1 - 2mr^{-1})[\mu^2 + (\lambda^2/r^2)(l - e\Phi)^2]. \tag{13}$$

The effective potential R is positive for $r > 2m$ and, as is evident from physical considerations, no particle can escape to infinity.

Since partial derivatives of the Jacobi action S with respect to the constants of motion, l, ϵ and μ, are themselves constants, the trajectories can be written in terms of quadratures. We give below one such integral corresponding to the differentiation with respect to l:

$$\phi = \int \frac{\lambda^4(l - e\Phi)}{r^2(\epsilon^2 - R)^{1/2}}\,\mathrm{d}r. \tag{14}$$

If we put $m = 0$ in (1), it represents Melvin's magnetic universe. By a simple transformation, the metric can be written in the form

$$\mathrm{d}s^2 = \lambda^2(\mathrm{d}\rho^2 + \mathrm{d}z^2 - \mathrm{d}t^2) + \rho^2\lambda^{-2}\,\mathrm{d}\phi^2 \tag{15}$$

where

$$\lambda = 1 + B^2\rho^2 \qquad \Phi = B\rho^2/\lambda. \tag{16}$$

Now the Hamilton–Jacobi equation reads

$$-\mu^2 = \lambda^{-2}[(S_\rho)^2 + \zeta^2 - \epsilon^2] + (\lambda^2/\rho^2)(l - e\Phi)^2 \tag{17}$$

which is already separated. The Jacobi action is given by

$$S = -\tfrac{1}{2}\mu^2\tau - \epsilon t + l\phi + \zeta z + S(\rho) \tag{18}$$

where

$$S(\rho) = \int (\epsilon^2 - R)^{1/2}\,\mathrm{d}\rho, \tag{19}$$

implying

$$\epsilon^2 \geqslant R \equiv \lambda^2\mu^2 + \zeta^2 + (\lambda^4/\rho^2)(l - e\Phi)^2 > 0. \tag{20}$$

Here ζ is the momentum along the z axis and R is the effective potential. As shown above, one can readily write the quadratures giving the trajectories.

3. Discussion

In the first four figures, we have plotted the effective potential R against r. We have set $\mu = 1$ throughout and, in addition, $m = 1$ for Ernst's field. All these plots and the other two diagrams of the orbits refer to the motion in the equatorial plane.

Figure 1 shows the effective potential curves for different values of l with fixed values of e and B. The Melvin universe (full curves) is compared with the test field (which is obtained by setting $\lambda = 1$ in the metric (15) and retaining Φ as in (16)) superposed on the flat space–time. The potential wells are narrower, meaning smaller regions for allowable motion, for the Melvin field than for the test field. The distinction between the two fields becomes quite marked for large values of l and/or r. In figure 2 the two fields are compared for varying field strengths with fixed e and l. The distinction is inappreciable for $B < 0{\cdot}05$ and starts increasing for large B. These two figures demonstrate the difference between geometrised (Melvin) and ungeometrised (test field) magnetic fields.

Figures 3 and 4 refer to potential curves in Ernst's field. In the former, l is varied while the latter is for varying B. We notice that, for $l < 5$, there are no potential wells, implying capture of particles by the black hole. The well starts developing for $l \geqslant 5$ and

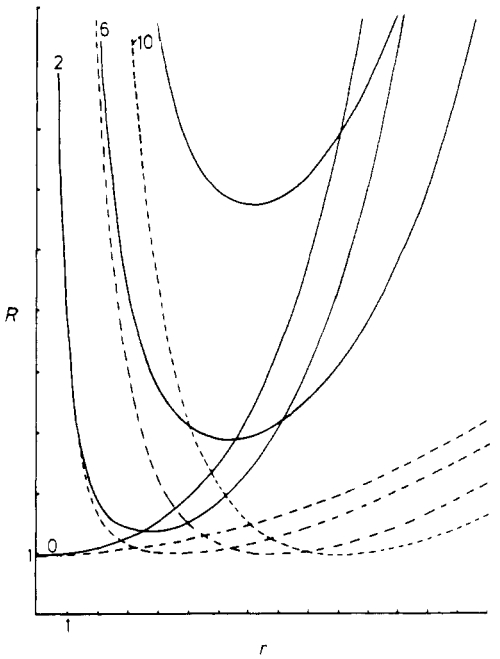

Figure 1. The equivalent potential curves for the Melvin universe (full curves) are compared with those for the test field (broken curves) ($\mu = 1$) for fixed $B = 0{\cdot}1$, $e = 1$ and various values of l (labels on curves).

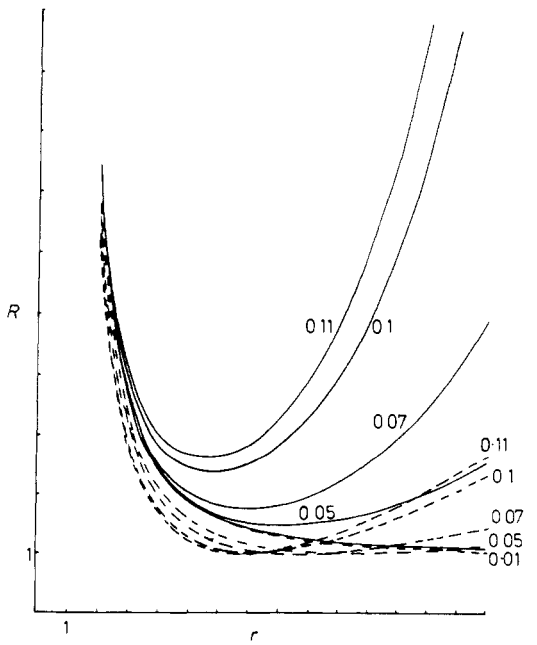

Figure 2. As figure 1, but with fixed $l = 5$, $e = 1$ and various values of B.

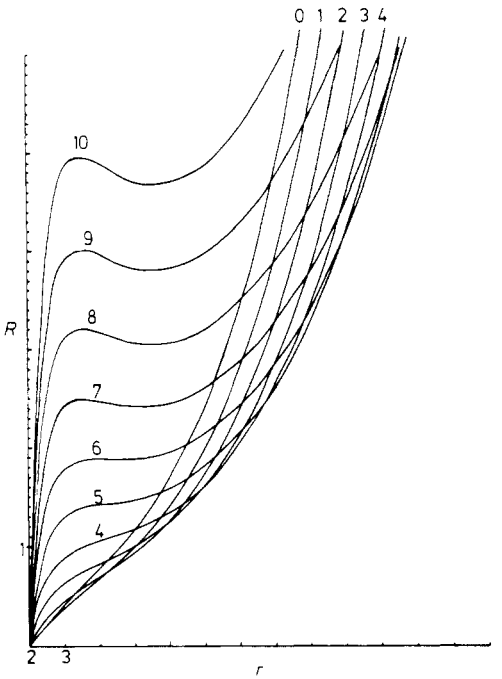

Figure 3. Ernst's field ($m = 1$, $\mu = 1$) for fixed $B = 0{\cdot}1$, $e = 1$ and various values of l.

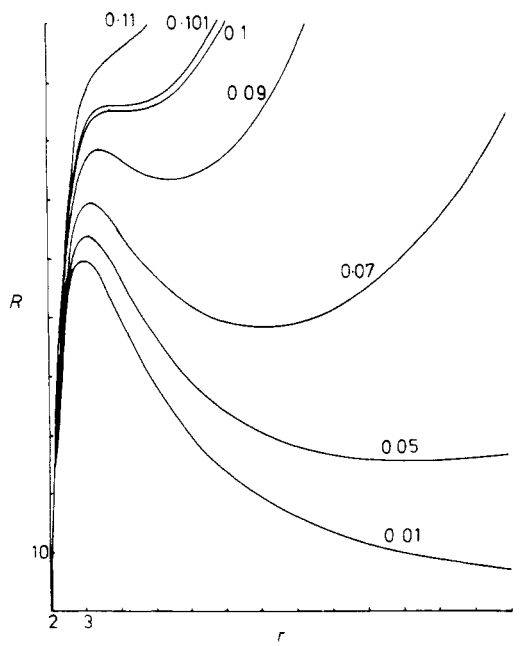

Figure 4. As figure 3, but with fixed $l = 40$, $e = 1$ and various values of B.

it goes on deepening and narrowing as l increases. Looking at the deepest points of the wells, we see that stable orbits could exist below 6 m. This means that the magnetic field pulls in the stability threshold of orbits. Figure 4 shows that bound orbits could exist for $B \leqslant 0{\cdot}101$ (equality refers to marginally bound orbits); for B larger than this, the particles will eventually be sucked in. These small values of B also correspond to the condition $|Bm| \ll 1$ under which space–time becomes approximately flat asymptotically and the magnetic field B uniform.

Figures 5 and 6 show two orbits. The former is a bound orbit where the particle's energy is appropriately chosen while the latter is a capture orbit where the energy is chosen so that it just skids over the well.

Figure 7 displays the cross section of the constant potential—Φ_M—lines (full curves) and the field lines (vertical broken lines) near the black hole. Though these lines do not

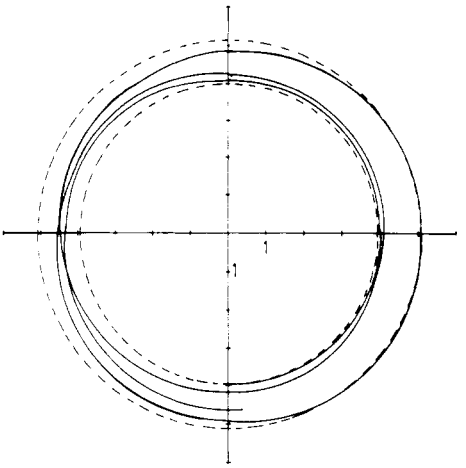

Figure 5. A bound orbit in the Ernst field, with parameters $l = 6$, $B = 0{\cdot}1$, $e = 1$ and $\epsilon^2 = 1{\cdot}881$. The broken circles mark the outer and inner boundaries of the orbit.

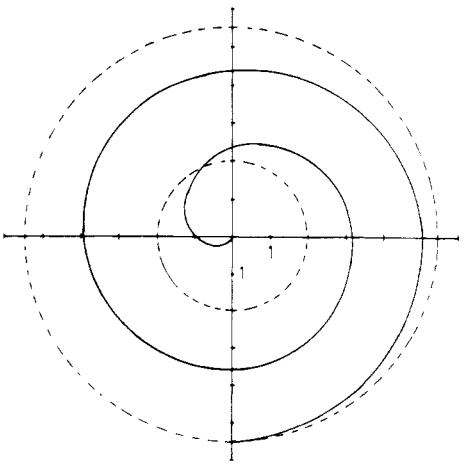

Figure 6. A capture orbit in the Ernst field, with parameters $l = 6$, $B = 0{\cdot}1$, $e = 1$ and $\epsilon^2 = 1{\cdot}9$. The broken circles indicate the outer boundary and the black hole.

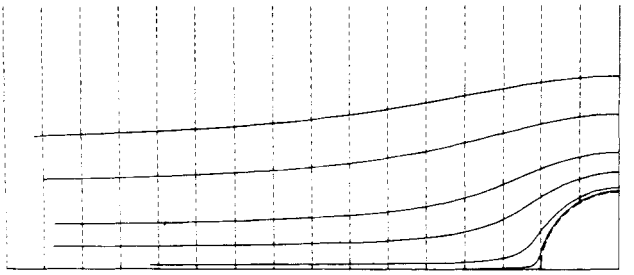

Figure 7. A quarter cross section of the constant potential lines (full curves) and the magnetic field lines (broken vertical lines) in the Ernst field.

appear to be orthogonal, they are in fact so, as can be verified from equations (5) and (6). It is interesting to note that the field lines remain unaffected by the introduction of a black hole in the Melvin universe.

Finally we comment on the order of magnitude of the magnetic field that determines the nature of the orbits. The conversion from dimensionless units to gauss is given by

$$B_G = \frac{c^4}{G^{3/2}M} B \simeq (2{\cdot}36 \times 10^{19}\,(M_\odot/M)B)\ \mathrm{G}.$$

We recall that for $l = 40$, the upper threshold for the existence of bound orbits is given by $B = 0{\cdot}1$. This value does not change appreciably for lower values of l. When converted to gauss, this limit corresponds to a rather high magnetic field, even in the case of supermassive black holes that are envisaged to be present in galactic nuclei, i.e. $B = 0{\cdot}1$ corresponds to $B_G \sim 10^{10}$ G for $M \sim 10^8\, M_\odot$. Therefore, bound orbits must exist for any realistic magnetic field. Thus a black hole immersed in such a field would be surrounded by a cloud of charged particles in bound orbits, though sufficiently energetic ones are sucked into the black hole.

Acknowledgments

Our collaboration is facilitated by financial support from the Raman Research Institute and the Centre for Theoretical Studies (Indian Institute of Science), Bangalore. CH thanks the former for the award of a fellowship while ND thanks both for a joint visiting fellowship. We also thank Mrs Jayanthi Ramachandran for helping us in numerical computations.

References

Carter B 1968 *Phys. Rev.* **174** 1559
Ernst F J 1976 *J. Math. Phys.* **17** 54
Melvin M A 1964 *Phys. Lett.* **8** 65